Chapter II

"Solution Structure of Ca^{2+}/CaM Complexed with its Binding Domain from Rat Ca^{2+}/CaM Dependent Protein Kinase Kinase Reveals a Novel Mode of Molecular Recognition"

II-1 Summary

The solution structure of calcium-bound calmodulin (Ca^{2+}/CaM) complexed with a 26-residue peptide corresponding to the CaM binding domain of rat Ca^{2+}/CaM dependent protein kinase kinase (CaMKK) has been determined by NMR spectroscopy. In the complex, the N-terminal region of the peptide adopts a helical conformation (Trp 444 to Leu 454) whereas the C-terminal forms a hairpin-like loop (Arg 455 to Ser 458). Residues Trp 444 and Phe 459 from the peptide, interact with the Ca^{2+}/CaM N and C-terminal hydrophobic pockets respectively. In addition the C-terminal Phe 463 side-chain plays a major role by interacting with Ile 448 and Leu 449 from its own peptide as well as hydrophobic residues in Ca^{2+}/CaM. These interactions stabilize the peptide's 'bent' conformation and indeed without Phe463, CaMKK cannot bind to Ca^{2+}/CaM. This means that in CaMKK 16 residues are used to link the two hydrophobic binding pockets of Ca^{2+}/CaM by adopting a conformation that is reminiscent of a 'walking-stick'. Longer than both the 14 residue region in MLCK and the 10 residue sequence from CaMKII, this motif defines a new mode of binding by requiring a longer motif, together with additional residues, to bind Ca^{2+}/CaM in the opposite orientation to that previously observed. These results provide an insight into how Ca^{2+}/CaM achieves broad target specificity in Ca^{2+} dependent signaling pathways.

II-2 Introduction

Calmodulin (CaM) dependent protein kinase kinase (CaMKK) regulates the upstream of a cascade that activates the kinases, CaM-kinase I (CaMKI) and IV (CaMKIV) (Lee & Edelman, 1994; Okuno & Fujisawa, 1993; Okuno *et al.*, 1994; Tokumitsu *et al.*, 1994; Tokumitsu *et al.*, 1995). Although calcium bound calmodulin (Ca^{2+}/CaM) is able to regulate CaMKI and IV directly, CaMKK phosphorylates CaMKI and IV, resulting in significant enhancement of the two enzymes.

CaMKK itself is autoinhibited by a sequence that occurs beyond the C-terminus of its kinase domain (Tokumitsu & Soderling, 1996). Site directed mutagenesis studies have identified the regulatory region of rat CaMKK between residues 435 and 463. This comprises an autoinhibitory domain (residues 435-440), and an overlapping CaM-binding domain (residues 438-463). It has been demonstrated that a synthetic peptide consisting of residues 438-463 is able to bind calmodulin in a Ca^{2+}-dependent manner, with a sub-nanomolar range dissociation constant (Tokumitsu *et al.*, 1997). With this information already available, further progress towards understanding the role of CaMKK in this cascade, would be assisted by knowing how Ca^{2+}/CaM binds to CaMKK.

Current understanding of the control mechanism for this pathway assumes an initially low Ca^{2+} concentration in the cytoplasm rising in response to a stimulus. Calcium-free CaM (apo CaM), which has until this time been in a closed conformation, binds calcium, resulting in a large conformational change (Ikura, 1996). During this change to the open conformation, hydrophobic residues that were previously buried in the core of the molecule become accessible. In this conformation CaM is now able to bind to target peptides such as the one in CaMKK. With the target peptide bound by Ca^{2+}/CaM and the autoinhibitory region extracted, the CaMKK active site is exposed and can interact with the downstream kinases; CaMKI and CaMKIV.

The next stage involves CaMKK phosphorylating a threonine residue in the activation loop of each CaMK, (Thr 177 in CaMKI and Thr 196 in CaMKIV) resulting in an increase in catalytic activity (Tokumitsu *et al.*, 1995). In turn, activated CaMKs efficiently phosphorylate their own physiological substrates until they are dephosphorylated and inactivated by a protein phosphatase (Aletta *et al.*, 1996; Tokumitsu *et al.*, 1994). Recent studies have revealed that one of the physiological functions of the CaMKK/CaMKIV cascade is transcriptional activation through phosphorylation of cAMP response element binding protein (CREB) at Ser 133 (Bading *et al.*, 1993; Bito *et al.*, 1996; Enslen *et al.*, 1994; Enslen *et al.*, 1995; Matthews *et al.*, 1994; Sun *et al.*, 1994).

Currently, structural data for the autoinhibition of Ca^{2+}/CaM dependent protein kinases and their subsequent activation by Ca^{2+}/CaM binding is limited. In fact, CaMKI is the only structure of which structure with an intact autoinhibitory region have been determined (Goldberg *et al.*, 1996). In this structure, the CaM binding site also overlaps the inhibitory region, suggesting that when CaM binds to the region it will simultaneously remove the inhibitory region away from the catalytic site, thereby activating the enzyme. For Ca^{2+}/CaM, the only known complexes are with peptides specifying the Ca^{2+}/CaM binding regions of CaMKII (Meador *et al.*, 1993) and myosin light chain kinase (MLCK, Ikura *et al.*, 1992; Meador *et al.*, 1992).

The overall sequence homology with other Ca^{2+}/CaM dependent protein kinases suggests that CaMKK is autoinhibited and activated by procedures similar to those observed in the related proteins described above. However there are several problems with this. Firstly there is no apparent similarity between the inhibitory loop sequences of CaMKI and CaMKK. As alternative methods of inhibition have already been revealed by the cAPK/PKI complex (Knighton *et al.*, 1991a; Knighton *et al.*, 1991b), there is no guarantee that CaMKK autoinhibition will follow either of these prototypes. Secondly, the

18

CaM binding peptide from CaMKK appears to be distinct, not only from the proposed CaM binding region of CaMKI, but also the motifs in CaMKII and MLCK, whose structure determinations have already shown distinct approaches to calmodulin binding (Figure II-1a). Taken together these results suggest that Ca^{2+}/CaM binding to the appropriate region of CaMKK, may use a hitherto unobserved approach.

As a step towards clarifying this situation, I decided to tackle this problem by determining the structure of Ca^{2+}/CaM bound to a synthetic peptide corresponding to the 26 residue region from CaMKK. This paper describes the structure determination of this Ca^{2+}/CaM complexed with CaMKK peptide by NMR spectroscopy. The binding mode is entirely unanticipated, having the opposite N-C polarity of all other known Ca^{2+}/CaM complexes and using a helix/hairpin loop combination that requires a longer sequence motif than previously observed.

II-3 Material and Method

II-3-1 Sample Preparation

A 26-residue synthetic peptide corresponding to the calmodulin binding domain of rat CaMKK was purchased from Peptide Institute Inc. and used without further purification. Uniformly ^{15}N- or ^{13}C/^{15}N-labeled recombinant *Xenopus laevis* CaM was expressed in *Escherichia coli* and purified to homogeneity as previously described (Ikura *et al.*, 1990a). CaM was dissolved in unbuffered 0.4 ml 95 % H_2O/5 % D_2O or 99.99 % D_2O solution containing 0.1 M KCl and 10mM $CaCl_2$. The pH/pD values of the samples were 6.7 without consideration of the isotope effects. The sample concentrations of CaM were 1.5 mM. The molar ratio of CaM and the CaMKK peptide was 1:1.25 for the sample used for the structure determination.

II-3-2 NMR Spectroscopy

All of the NMR spectra were measured at 30 °C on a Bruker AMX-600 spectrometer. CaMKK was titrated in aliquots of 0.25 protein equivalent into a uniformly ^{15}N-labeled sample of the protein. After the addition of each aliquot of the peptide, 1D ^{1}H, and 2D ^{15}N-^{1}H HSQC (Kay *et al.*, 1992; Palmer III *et al.*, 1991) were acquired. Finally, spectra with 0, 0.25, 0.50, 1.0, and 1.25 equivalents of CaMKK peptide to CaM were recorded.

Sequential assignments of the backbone resonances of CaM were achieved by the sets of experiments, HNCACB (Wittekind & Mueller, 1993) and CBCA(CO)NH (Grzesiek & Bax, 1992a; Szyperski *et al.*, 1994), CT-HNCO (Grzesiek & Bax, 1992b), gd-HCACO (Zhang & Gmeiner, 1996), ^{15}N-edited TOCSY-HMQC, HNHA (Vuister & Bax, 1993) and HBHA(CBCACO)NH (Grzesiek & Bax, 1993). Side-chain assignments were obtained from H(CCO)NH (Grzesiek *et al.*, 1993), C(CO)NH (Grzesiek *et al.*, 1993), and HCCH-TOCSY (Bax *et al.*, 1990) experiments.

The assignments of the CaMKK peptide were obtained by $[^{15}N/F_2]$-filtered NOESY, $[^{15}N/F_2]$-filtered TOCSY, $[^{13}C,^{15}N/F_2]$-filtered NOESY, $[^{13}C,^{15}N/F_2]$-filtered TOCSY, $[^{13}C/F_1,F_2]$-filtered NOESY, $[^{13}C/F_1,F_2]$-filtered TOCSY, and $[^{13}C/F_1,F_2]$-filtered COSY. The mixing times of these filtered spectra was 50 ms, 100 ms, and 200 ms for NOESY and 35 ms, 50 ms, 60 ms, and 70 ms for TOCSY, respectively. In all the NMR experiments for the samples dissolved in H_2O, water suppression was achieved using the WATERGATE technique (Piotto et al., 1992). The experimental details are the same as previously reported (Ames et al., 1994). All data were processed using the software nmrPipe and nmrDraw (Delaglio, 1993; Delaglio et al., 1995), and the data analysis was assisted by the software Pipp (Garrett et al., 1991).

The sequence specific assignments for the rat CaMKK peptide bound to Ca^{2+}/CaM were carried out by analyzing a series of isotope filter experiments based on NOE connectivities. My data showed distinct peaks at 9.7 ppm in the $[^{13}C,^{15}N/F_2]$-filtered NOESY experiment (Figure II-2a), which are usually indicative of a proton bound to a Trp side-chain indole nitrogen. However, the similar spectra of the homologous C. elegans peptide, which has no Trp residues and a Leu residue at the position corresponding to rat CaMKK, Trp 444, showed the identical peaks, confirming that they must correspond to a conserved aromatic group (Figure II-2b). With this information available, sequential assignments for the peptide were made without any difficulty and the previously discussed peaks were assigned to Phe 459.

Slowly exchanging amide protons were identified by monitoring the $^1H/D$ exchange rate of the backbone amides from a series of sensitivity-enhanced $^{15}N-^1H$ HSQC spectra recorded at different time points (19, 38, 54, 87, 120, 185, 319, 459, 600, and 793 min) immediately after dissolving the lyophilized Ca^{2+}/CaM complexed with the CaMKK peptide in D_2O. The backbone coupling constants, $^3J_{NH\alpha}$, were measured from a HNHA experiment

(Vuister & Bax, 1993). Stereospecific assignments of valine and leucine methyl groups were obtained by analyzing a constant time ^{13}C-^1H HSQC spectrum of 10 % ^{13}C-enriched Ca^{2+}/CaM complexed with CaMKK peptide (Neri *et al.*, 1989). The ^1H, ^{13}C, and ^{15}N resonance assignments has been deposited with the BioMagResBank, with accession number of 4270.

II-3-3 Structure Calculation

Approximate interproton distances were obtained from ^{13}C-edited NOESY-HMQC (Ikura *et al.*, 1990b), ^{15}N-edited NOESY-HMQC (Marion *et al.*, 1989), [^{13}C/F_3]-filtered [^{13}C/F_1]-edited HMQC-NOESY (Lee *et al.*, 1994), [^{15}N/F_2]-filtered NOESY [^{13}C,^{15}N/F_2]-filtered NOESY and [^{13}C/F_1,F_2]-filtered NOESY. The mixing time was 100 ms for all NOESY experiments. The distance restraints were grouped into four classes: 1.8-2.7, 1.8-3.3, 1.8-5.0, and 1.8-6.0 Å corresponding to strong, medium, weak, and very week NOE cross-peak intensities, respectively. The NOEs including backbone amide protons were grouped into four classes of 1.8-2.9, 1.8-3.5, 1.8-5.0, and 1.8-6.0 Å. ϕ and ψ dihedral angle restraints were derived from the $^3J_{NH\alpha}$ coupling constants and chemical shift indices (Wishart & Sykes, 1994). Values of -60° ± 30° and -40° ± 30° were used for ϕ and ψ dihedral angles, respectively, for α-helical regions; -120° ± 50° and 120° ± 50° for β-strands. Hydrogen bond restraints were obtained by analyzing the ^1H/D exchange rates and the NOE patterns characteristic of α-helices or β-strands. Two distance restraints, r_{NH-O}(0-2.3 Å) and r_{N-O}(0-3.3 Å), were used for each hydrogen bond. Structures were calculated using the YASAP protocol (Nilges *et al.*, 1988) within X-PLOR (Brünger, 1992) as previously described (Bagby *et al.*, 1994). The final structures were calculated based on 2541 interproton distance restraints (823 intraresidue, 468 sequential, 337 short-range, 362 long-range for CaM, 150

intraresidue, 65 sequential, 29 short-range, 20 long-range for CaMKK peptide, and 271 intermolecular), 112 distance restraints for hydrogen bonds, 24 distance restraints for four Ca^{2+} coordinations, and 115 dihedral angle restraints. The coordinates for the final structures and structural constraints used in the calculations have been deposited with the Protein Data Bank, Chemistry Department, Brookhaven National Laboratory, NY 11973 USA, with accession code of 1CKK.

II-3-4 Site-directed Mutagenesis

COS-7 cells were maintained in Dulbeco's modified Eagle's medium containing 10 % fetal calf serum. Cells were subcultured in 10 cm dishes 12 hours before transfection. The cells were then transferred to serum-free medium and treated with a mixture of either 10 mg of pME18s plasmid DNA (DNAX Research Institute, Inc.) or CaMKK cDNA containing plasmid DNAs and 60 mg of LipofectAMINE Reagent (Life Technologies, Inc.) in 6.8 ml of medium.   After 32-48 hours incubation, the cells were collected and homogenized with 1 ml of lysis buffer (150 mM NaCl, 20 mM Tris·HCl, pH 7.5, 1 mM EDTA, 1% NP-40, 10% glycerol, 0.2 mM PMSF, 10 mg/l leupeptin, 10 mg/l pepstatin A, 10mg/l trypsin inhibitor) at 4 °C. After centrifugation at 15,000 g for 15 min, each transfected cell extract (18 mg) was analyzed by both Western blotting using anti CaMKK antibody (Transduction Lab.) and biotinylated CaM-overlay.

II-4 Results and Discussion

II-4-1 NMR Spectroscopy

Tokumitsu *et al.* indicated that the region between residues 438 and 463 of CaMKK was sufficient to bind to Ca^{2+}/CaM. Furthermore, using site directed mutagenesis it had also been shown that mutations at 455-457 significantly reduced Ca^{2+}/CaM binding activity (Tokumitsu *et al.*, 1997). In addition, they have constructed two more mutants, F459D and F463D, both of which resulted in total loss of CaM binding (Figure II-1b). Taken together, I decided to use a peptide corresponding to residues 438-463 of rat CaMKK for NMR structure determination. A corresponding peptide encoding *C. elegans* CaMKK (347-372) is also synthesized and compared by NMR (Figure II-1a and see later). These CaMKK peptides by themselves are unstructured, as evidenced by NMR spectroscopy (data not shown). However, the peptides adopt a single folded conformation upon complexation with Ca^{2+}/CaM (Figure II-2). Such induced folding has been seen previously in the CaM-MLCK peptide (M13) complex (Ikura *et al.*, 1992), and is becoming a common theme in molecular recognition events including protein-protein (Radhakrishnan *et al.*, 1997), protein-DNA (Spolar & Record, 1994), and protein-RNA (Frankel & Smith, 1998) interactions. In accordance with the induced folding process of the CaMKK peptide upon complexation with Ca^{2+}/CaM, the NMR spectra of CaM also change upon binding to the CaMKK peptide. During a titration experiment in which ^{15}N-^{1}H HSQC spectra of CaM were recorded with successive additions of the CaMKK peptide, most peaks corresponding to the peptide-free state decrease in intensity and appear at new positions corresponding to the peptide-bound state. This slow-exchange phenomenon is consistent with the high affinity of the CaMKK peptide for CaM ($K_d \sim 10^{-9}$M, Tokumitsu *et al.*, 1997).

24

II-4-2 Structure Description

The three-dimensional structure of Ca^{2+}/CaM complexed with the CaMKK peptide has been determined using 2525 NOE-based distance restraints including 271 intermolecular restraints, supplemented with 115 dihedral and 112 hydrogen bond restraints. The best-fit superposition of backbone atoms for 30 models, together with ribbon and stick diagram of the averaged structure, is shown in Figure II-3. A summary of the structural statistics is given in Table II-1.

As seen in the CaM-M13 complex (Ikura *et al.*, 1992; Meador *et al.*, 1992), the 'central helix' undergoes partial melting upon binding the CaMKK peptide, resulting in a flexible loop comprising residues 74-82. This change in the domain linker enables the two domains to come together to clamp the CaMKK peptide in a manner globally similar to that of the CaM-M13 (Ikura *et al.*, 1992; Meador *et al.*, 1992) and CaM-CaMKII (Meador *et al.*, 1993) complexes. However it is here that resemblance to other structures of CaM-peptide complexes ends. Unlike the previously known CaM-bound target peptide forming α-helix to bind to CaM, the CaMKK peptide consists of two structural segments involved in the interaction with CaM (Figure II-4); a 11-residue long α-helix (residues 444-454), and a hairpin-like loop structure (residues 455-459). The N-terminal portion of the peptide helix provides Trp 444, a key hydrophobic residue that anchors the peptide helix to the N-terminal domain of CaM (Figure II-5a). The C-terminal domain interacts with both the C-terminal portion of the helix and the hairpin loop. Unexpectedly, Phe 459 in the hairpin loop serves as another key residue to anchor the peptide to the C-terminal domain of CaM (Figure II-5b).

The hairpin loop structure is stabilized by electrostatic interactions involving three basic residues, Arg 455, Lys 456, and Arg 457. These positively charged residues are in close proximity with the negatively charged residues of CaM, Glu 14, Glu 120, Glu 123, and Glu 127, such that they could

contribute to intermolecular interactions. In addition, intramolecular hydrophobic interactions involving Phe 463, Ile 448 and Leu 449 (Figure II-6). These residues also contact intimately with Met 72 and Met 76 of CaM. The ability to bind to CaM is impaired in the F463D mutant, presumably due to distortion of these hydrophobic interactions involving Phe 463.

II-4-3 Variable Domain Orientation

The relative position and distance between the N and C-terminal domains of CaM complexed with the CaMKK peptide differ from those observed in other CaM-peptide complexes (Ikura *et al.*, 1992; Meador *et al.*, 1992; Meador *et al.*, 1993). The differences can be quantitatively analyzed by R.M.S. deviation values for backbone superpositions between the individual domains of all three complexes (the values without parentheses in Table II-2). The R.M.S. deviation value (1.79 Å) between CaMKK and MLCK complexes is smaller than that (2.59 Å) between CaMKK and CaMKII complexes, consistent with the difference in the size of spacer between the two key hydrophobic residues of the target peptides: the 16-residue spacer of the CaMKK complex, the 14-residue spacer of the MLCK complex, and the 10-residue spacer of the CaM-CaMKII peptide complex. In general, the complementality of the molecular shape is essential for the hydrophobic interaction. However, the results obtained here indicate that the relative orientation, i.e., the shape of the hydrophobic channel of CaM can be optimized by the interaction with the target peptide due to the high flexibility of the domain linker of CaM, which contributes to the broad specificity of CaM molecular recognition.

II-4-4 Peptide Polarity

Another striking difference of this structure with other structures of CaM-peptide complexes concerns the direction of the peptide helix axis with respect to the CaM two domains. In all previously known cases (i.e., CaM-skMLCK peptide, CaM-smMLCK, CaM-CaMKII), the peptide helix is oriented in one direction such that the N-terminal portion binds to the C-terminal domain of CaM, while the C-terminal portion to the N-terminal domain of CaM (Figures II-7b and c). Surprisingly, the peptide orientation is reversed in the case of the CaM-CaMKK peptide complex, as described above and illustrated in Figure II-7a. What determines the orientation of the target helix with respect to the CaM molecule?

(a) Steric factor

It has been already reported that both CaM domains of the CaM-MLCK complex are related by a two fold symmetry, suggesting that the target peptide could bind Ca^{2+}/CaM in both orientations (Meador *et al.*, 1992). The superposition in a reversed orientation (i.e. the N-terminal domain of one complex and the C-terminal domain of the other complex, and vice versa, the values in parentheses in Table II-2) of the CaM-MLCK complex itself give rise to the lowest value of 0.84 Å among those calculated here, indicating that the domains are symmetrically related. Although the symmetry is lost for the CaM-CaMKK complex (2.53 Å) and the CaM-CaMKII complex (2.53 Å), the small value (1.14 Å) is obtained when the CaM-CaMKK structure is superimposed with the CaM-CaMKII structure in a reversed orientation. These results confirm that the CaM N and C-terminal domains are structurally similar to each other and could be interchanged without causing steric hindrance with the bound target peptide, suggesting that the binding polarity could be mainly determined by the factors other than van der Waals interaction.

27

(b) Electrostatic Factor

Further close examination of this structure together with other CaM-peptide complex structures led me to an interesting observation on the characteristic of the hydrophobic channel composed by the CaM two domains. As noted previously (Afshar *et al.*, 1994; Meador *et al.*, 1992; Meador *et al.*, 1993), electrostatic interactions play a role in the interaction of CaM with target peptides. At the two opposite outlets of the hydrophobic channel are clusters of acidic residues that are asymmetric in size. In the view shown in Figure II-8, a significantly large number of acidic residues cluster at the right outlet of the channel than the left outlet, resulting in electrostatic polarity of the channel. Not surprisingly, CaM target peptides that interact with this channel possess complementary polarity created by a cluster of basic residues in the amino acid sequence (Figures II-8 and 9). Interestingly, the basic cluster of CaMKK is located at the C-terminal side of the CaM-binding region, while that of MLCK and CaMKII at the N-terminal side (Figure II-9). These differences in amino acid sequence are consistent with the polarity of peptide in the known structures.

(c) Prediction of the Peptide Polarity

These observations indicate that the location of a basic cluster within the CaM-binding region of target proteins play an important role in determining the direction of its binding with respect to CaM domains. This suggests that one can predict which orientation is preferred for certain target protein when it binds to CaM. Based on the sequence comparison (Figure II-9), CaMKI and IV, calspermin and calcineurin all bind to CaM in the orientation same as that seen in MLCK and CaMKII. On the other hand, *C. elegans* CaMKK, *D. melanogaster* myosin ninaC (neither inactivation nor afterpotential C), *M. Domestica* CaMK, and rat guanine nucleotide releasing protein (GNRP) use the orientation observed in the structure of rat CaMKK complexed with CaM.

28

However, it should be noted that there are some cases, including caldesmon (Rhoads & Friedberg, 1997), in which no basic cluster is recognizable.

(d) Comparison with the SH3 and Proline-rich Peptide

The dual binding orientations of the peptide, which may be determined by the position of the basic residues, are similar to the binding of proline-rich peptide to Src-homology-3 (SH3) domains (Lim et al., 1994; Saraste & Musacchio, 1994). In the complex, the proline-rich peptide adopts a conformation called the polyproline II helix (PPII), in which a sequence pattern such as PXXP place two prolines on the same side of a PPII helix. Due to the pseudo-symmetric nature of the PPII structure, it could bind to SH3 domain in both orientation without causing a large conformational change in the SH3 domain. Thus, the binding orientation of the peptide was suggested to be mainly determined by the electrostatic interaction between Arg residue before or after the PXXP core in the proline-rich peptide and a conserved carboxylic acid in the RT-loop of the SH3 domain. This contribution of the electrostatic interaction to the binding polarity seems similar to that to the binding of the target peptide to Ca^{2+}/CaM.

However, only one side of the PPII helix is recognized by the SH3 domain on its surface, leading to the affinity typically in the 10^{-4}~10^{-6} M range (Cussac et al., 1994; Viguera et al., 1994; Yu et al., 1994). This low binding affinity may be important for turning its signal on and off without undergoing a large structural change in the SH3 domain. On the other hand, Ca^{2+}/CaM undergoes a large structural change upon complexation with its target peptide. This structural adaptation makes it possible for Ca^{2+}/CaM to acquire two contradictory properties: the high affinity (10^{-7}~10^{-10} M) and the target diversity. It should be noted that the acidic residues of each CaM domain interacting with the basic residues of the target peptide come close together in the complex structures (Figure II-8). This suggests that the basic residues in

the peptide play a role in stabilizing the globular structures by canceling the electrostatic repulsion between both domains, which might determine the peptide polarity in the early stage of the recognition process.

II-4-5 Correlation with Mutagenesis Studies

The structure of the CaM–CaMKK peptide complex is consistent with previous mutagenesis studies on CaMKK (Tokumitsu *et al.*, 1997). Both block-aspartate-scanning and point mutagenesis were used to mutate four nonoverlapping blocks and two single sites of amino acids within the putative CaM-binding region of CaMKK (residues 435-463). Of the four block mutants, those involving residues 443-445, 448-450 and 455-457 exhibited drastic effects in Ca^{2+}/CaM sensitivity of the CaMKK enzymatic activity. The former two regions correspond to the helix and the latter one to the hairpin loop, which are all crucial to the CaM–CaMKK interaction. A block mutant involving residues 438-440, on the other hand, showed no effects on the Ca^{2+}/CaM sensitivity. Indeed, this region is not involved in the direct contact with CaM. Point mutations to aspartate involving Phe 459 and Phe 463, both resulted in dramatic effects on the Ca^{2+}/CaM sensitivity. These residues, located at the hairpin loop, are involved in interactions with the C-terminal domain of CaM.

A recent mutagenesis study (Matsushita & Nairn, 1998) indicated that a truncated mutant of $CaMKK_{1-457}$ retains Ca^{2+}/CaM sensitivity in the phosphorylation activity. This is not surprising since a majority of residues (16 out of 22) involved in the intimate CaM–CaMKK interaction (Figure II-4) is included in the mutant thereby maintaining the ability to bind to Ca^{2+}/CaM. However, the lack of residues 458-463 should have an impact on the Ca^{2+}/CaM dependent activation of the enzyme: the $CaMKK_{1-457}$ mutant is expected to

have less affinity with the C-terminal domain of CaM than the wild-type protein.

II-5 Concluding Remarks

The detection of a new binding mode of CaM-target interactions raises a question concerning how many ways are used by Ca^{2+}/CaM to recognize target proteins. The present structure provides an example in which a target peptide helix can bind the N and C-terminal domains of CaM with a polarity opposite to that observed for the CaM-MLCK and CaM-CaMKII complexes. Furthermore, it is not only the 11-residue long helix but also a hairpin loop that is involved in the interaction with CaM. Clearly, by virtue of the two-domain architecture and the flexible domain linker, CaM uses various conformations and binding schemes to confer broad specificity. I predict to see new structures of CaM-target complexes that differ significantly from those reported so far.
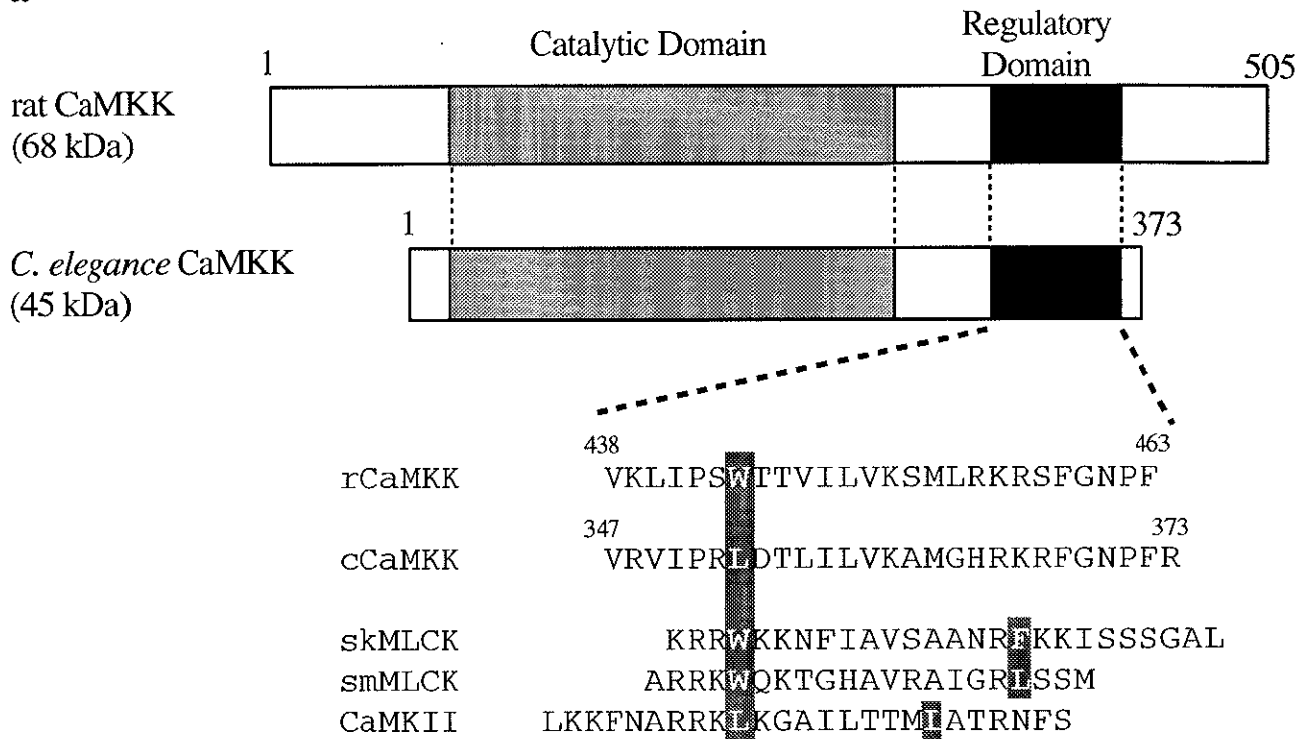
Figure II-1. a, Alignment of Ca^{2+}/CaM binding sequences of CaMKKs, MLCKs, and CaMKII based primarily on the key hydrophobic residues (white) binding to the hydrophobic pockets of Ca^{2+}/CaM.

Sequences: rat CaMKK (rCaMKK, residues 438–463, Tokumitsu *et al.*, 1997), *C.elegans* CaM–KK (cCaMKK, residues 347–373, Tokumitsu *et al.*, manuscript in submitted), skeletal muscle MLCK (skMLCK, residues 342–367, Ikura *et al.*, 1992), smooth muscle MLCK (smMLCK, residues 796–815, Meador *et al.*, 1992), and CaMKII (residues 290–315, Meador *et al.*, 1993).
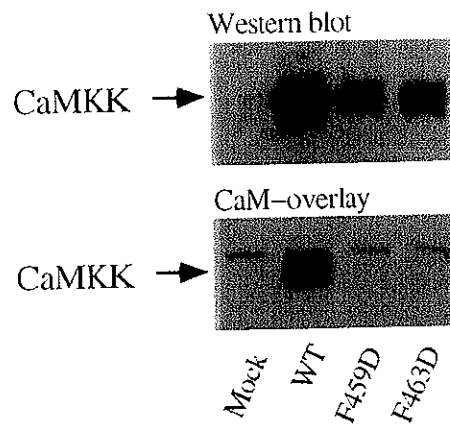
b

Figure II-1. b, Binding of CaMKK mutants (F459D and F463D) to Ca^{2+}/CaM. COS-7 cells were maintained in Dulbeco's modified Eagle's medium containing 10 % fetal calf serum. Cells were subcultured in 10 cm dishes 12 hours before transfection. The cells were then transferred to serum-free medium and treated with a mixture of either 10 mg of pME18s plasmid DNA (DNAX Research Institute, Inc.) or CaMKK cDNA containing plasmid DNAs and 60 mg of LipofectAMINE Reagent (Life Technologies, Inc.) in 6.8 ml of medium. After 32–48 hours incubation, the cells were collected and homogenized with 1 ml of lysis buffer (150 mM NaCl, 20 mM Tris–HCl, pH 7.5, 1 mM EDTA, 1 % NP–40, 10 % glycerol, 0.2 mM PMSF, 10 mg/l leupeptin, 10 mg/l pepstatin A, 10 mg/l trypsin inhibitor) at 4 °C. After centrifugation at 15,000 g for 15 min, each transfected cell extract (18 mg) was analyzed by both Western blotting (Upper panel) using anti CaMKK antibody (Transduction Lab.) and biotinylated CaM–overlay (Lower panel).
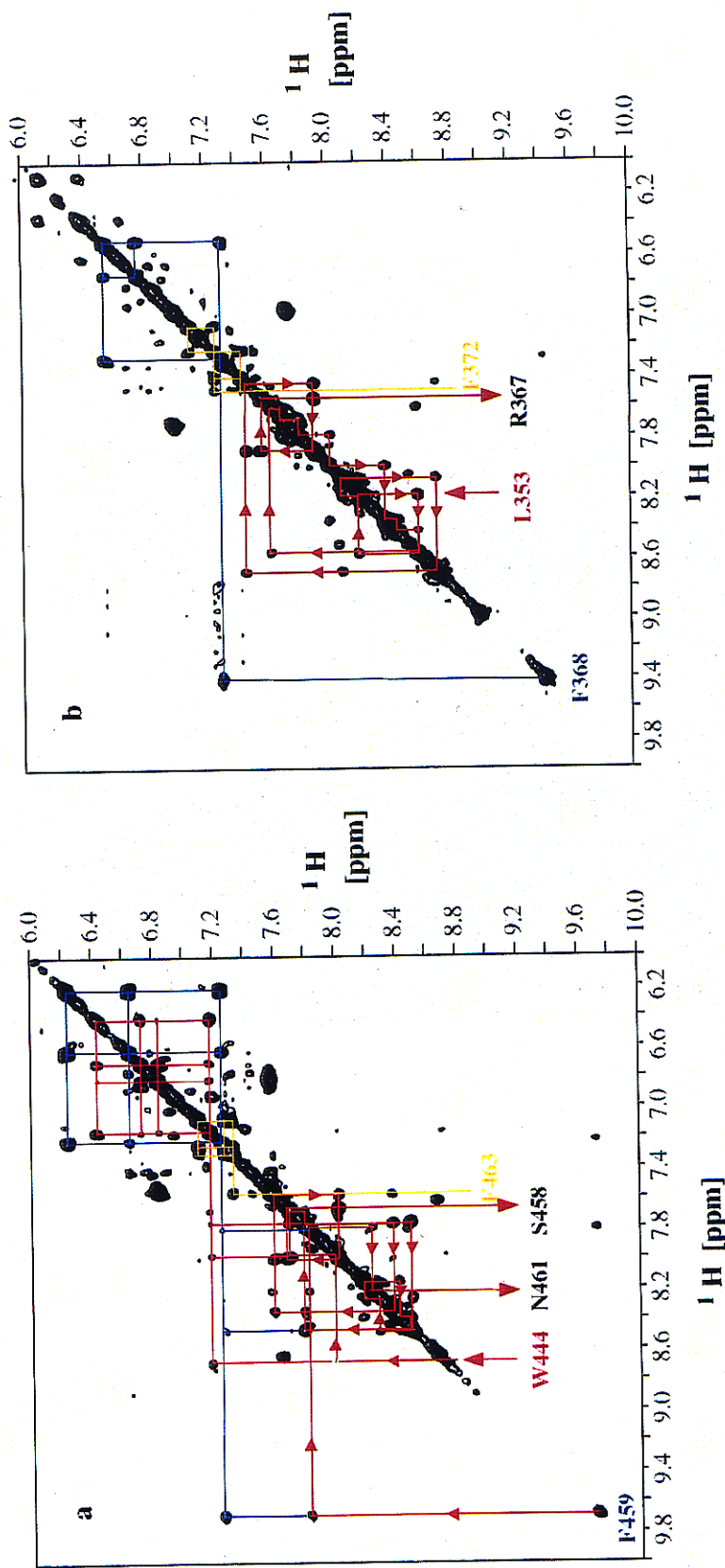
Figure II–2. Amide and aromatic region of [^{13}C, $^{15}N/F_2$]–filtered NOESY spectra for the CaMKK peptide from a, rat and b, *C. elegans* in complex with Ca^{2+}/CaM. The sequential assignments were carried out based on the NOE connectivities.
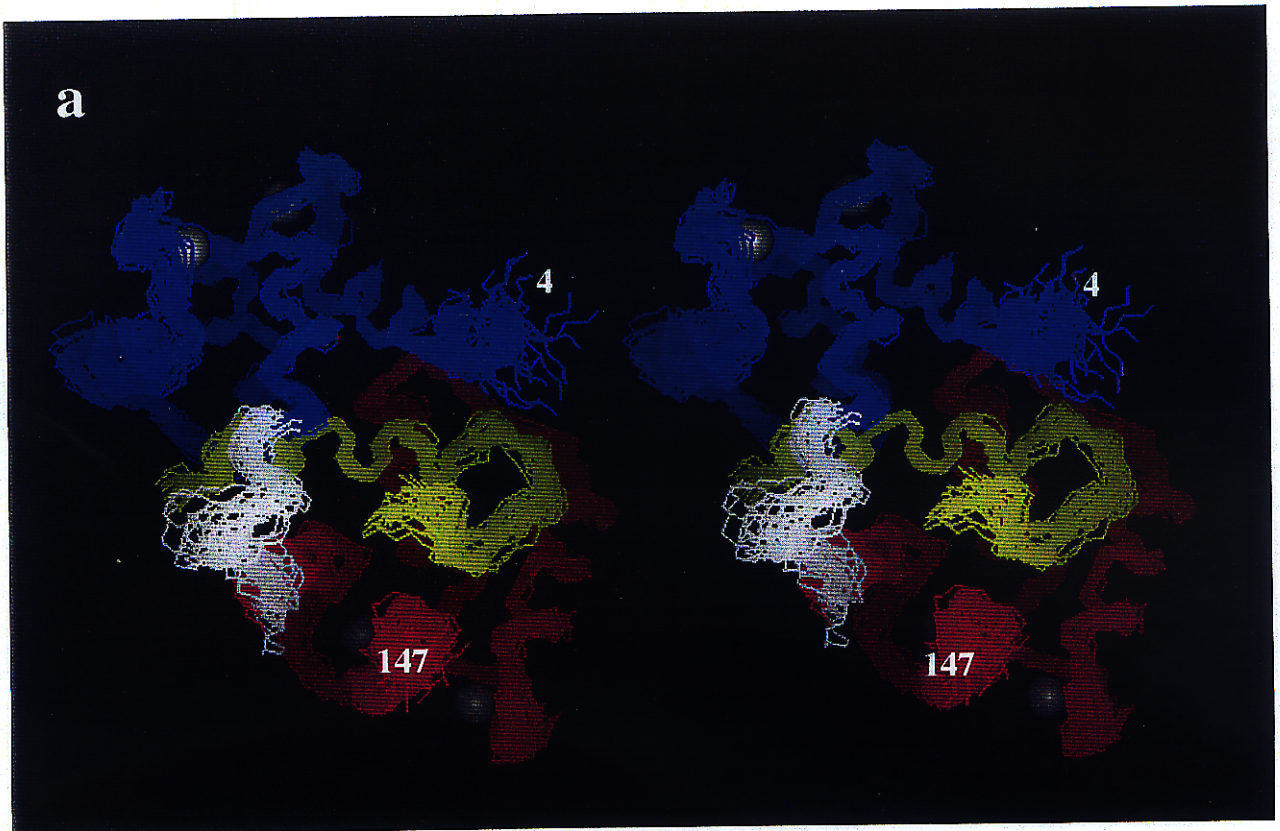
Figure II–3. a, Stereo drawing of the 30 NMR models showing Ca^{2+}/CaM (N and C–terminal domains are shown in blue and magenta, respectively) and the rat CaMKK peptide (yellow). Each model was superimposed onto the energy–minimized average structure using residues 6–18, 26–39, 45–55, 62–74, 83–91, 99–111, 118–127, 135–146 of CaM and 443–463 of CaMKK. When using only backbone atoms (N, C, and C) the R.M.S. deviation was 0.78 ± 0.06 Å. For all heavy atoms (not shown) this increased to 1.38 ± 0.06 Å. This figure was generated using Insight II (Biosym, San Diego, CA).
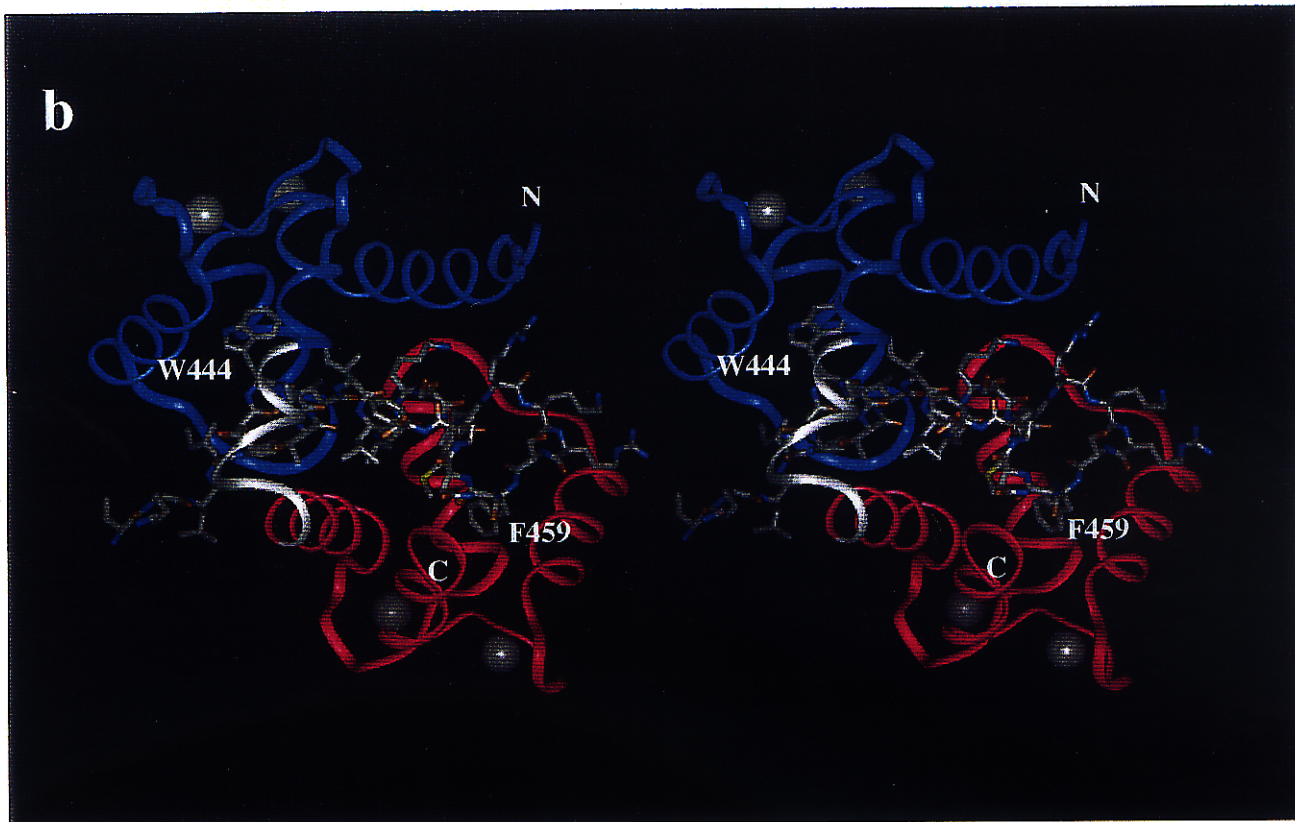
Figure II–3. b, Ribbon (CaM) and stick (CaMKK) drawing of the energy–minimized average structure. Carbon, nitrogen, oxygen and sulfur aroms of CaMKK are colored in white, blue, orange, and yellow, respectively. This figure was generated using Insight II (Biosym, San Diego, CA).

Table II-1. Structural statistics of the 30 structures of Ca^{2+}/CaM complexed with the CaMKK peptide[1]

R.M.S. deviations from experimental distance restraints (Å)	
All (2563)	0.018 ± 0.000
Interresidue sequential NOE ($|i - j| = 1$) (535)	0.022 ± 0.003
Interresidue short range NOE ($1 < |i - j| \leq 5$) (366)	0.020 ± 0.012
Interresidue long range NOE ($|i - j| > 5$) (382)	0.008 ± 0.002
Intraresidue NOE (973)	0.013 ± 0.005
Intermolecular NOE (285)	0.023 ± 0.002
Hydrogen bond (112)	0.022 ± 0.002
R.M.S. deviations from experimental dihedral restraints (deg) (201)	
	0.08 ± 0.04
R.M.S. deviations from idealized geometry	
Bonds (Å)	0.003 ± 0.000
Angles (deg)	0.49 ± 0.01
Impropers (deg)	0.36 ± 0.00
Energies (kcal mol^{-1})	
$F_{NOE}{}^{2}$	41.85 ± 6.36
$F_{cdih}{}^{2}$	0.090 ± 0.119
$F_{repel}{}^{3}$	9.08 ± 2.58
$F_{L-J}{}^{4}$	-317.6 ± 48.3

[1]The number of each type of restraints used in the structure calculation is given in parenthesis. None of the structures exhibits distance violations greater than 0.5 Å or dihedral angle violations greater than 2.6 deg.

[2]F_{NOE} and F_{cdih} were calculated using force constraints of 50 kcal mol^{-1} Å^{-2} and 200 kcal mol^{-1} rad^{-2}, respectively.

[3]F_{repel} was calculated using a final value of 4.0 kcal mol^{-1} Å^{-4} with the van der Waals hard sphere radii set to 0.75 times those in the parameter set PARALLHDG supplied with X-PLOR (Brünger, 1992).

[4]E_{L-J} is the Lennard-Jones van der Waals energy calculated with the CHARMM empirical energy function and is not included in the target function for simulated annealing calculation.
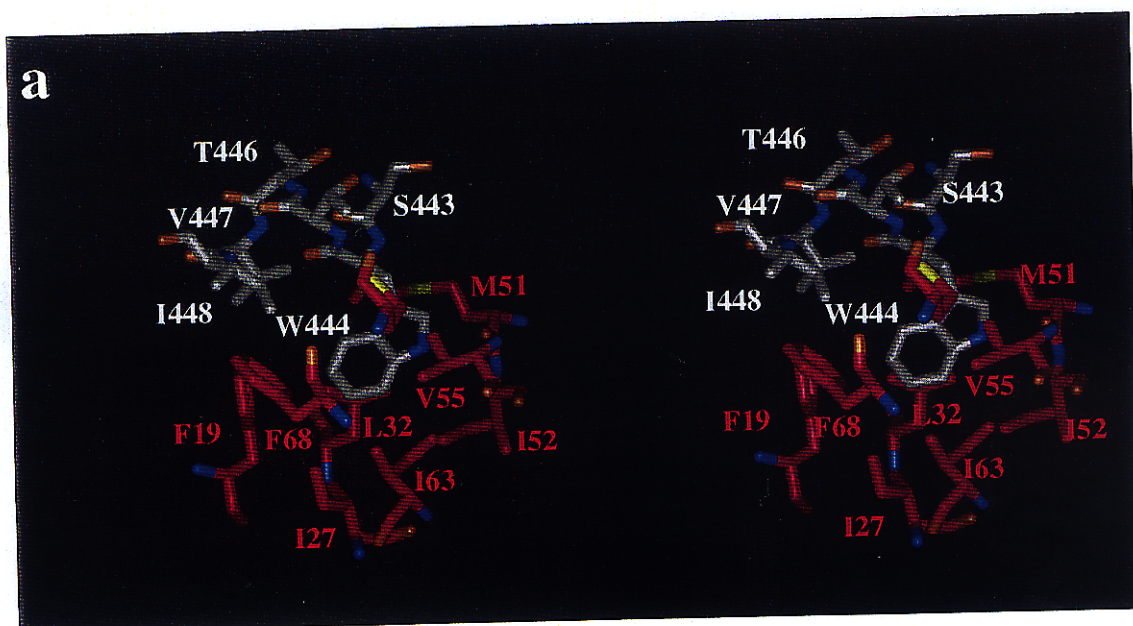
Figure II–4. Schematic drawing of interacting residues between Ca^{2+}/CaM and CaMKK peptide. Residues in N and C–terminal domain of Ca^{2+}/CaM are colored in blue and magenta, respectively. Key residues of the CaMKK peptide anchoring the hydrophobic pocket in each domain, Trp 444 and Phe 459, are shown in green.

38

Figure II–5. a. Stereo drawing of the key residues of the CaMKK peptide bound to the hydrophobic pocket of the N–terminal domain of CaM. Residues within 5 Å of the N–terminal key residue, Trp 444, are shown. Nitrogen, oxygen and sulfur atoms are colored in blue, orange, and yellow, respectively, while carbon atoms of CaM and CaMKK are shown in magenta and white, respectively. This figure was generated using Insight II (Biosym, San Diego, CA).
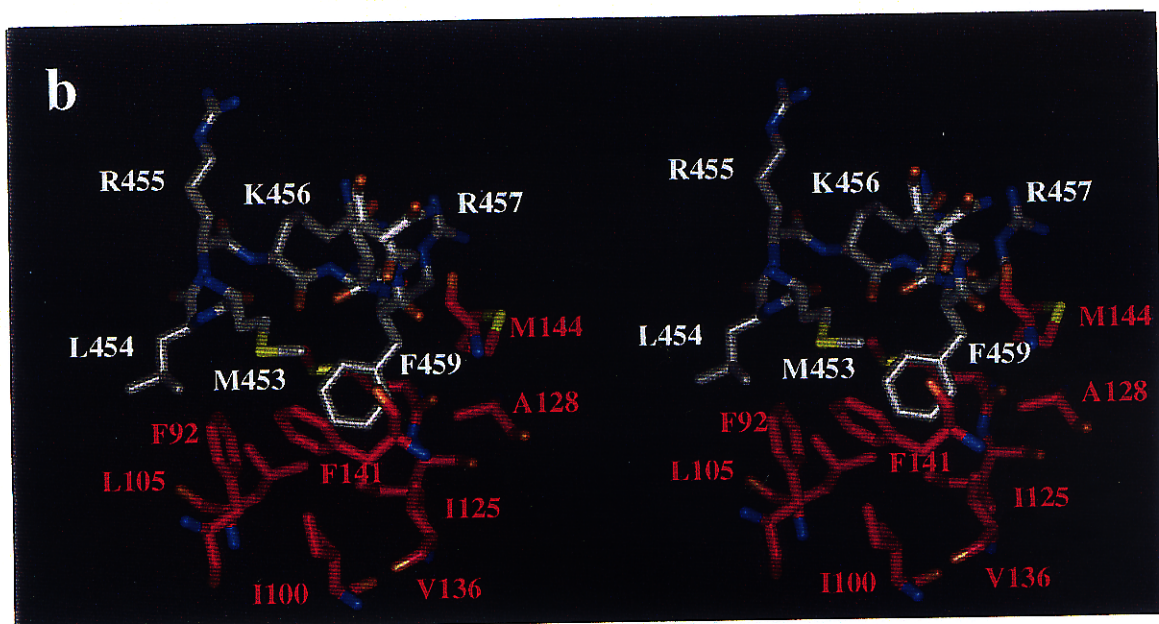
Figure II–5. b, Stereo drawing of the key residues of the CaMKK peptide bound to the hydrophobic pocket of the C–terminal domain of CaM. Residues within 5 Å of the C–terminal key residue, Phe 459, are shown. Nitrogen, oxygen·and sulfur atoms are colored in blue, orange, and yellow, respectively, while carbon atoms of CaM and CaMKK are shown in magenta and white, respectively. This figure was generated using Insight II (Biosym, San Diego, CA).
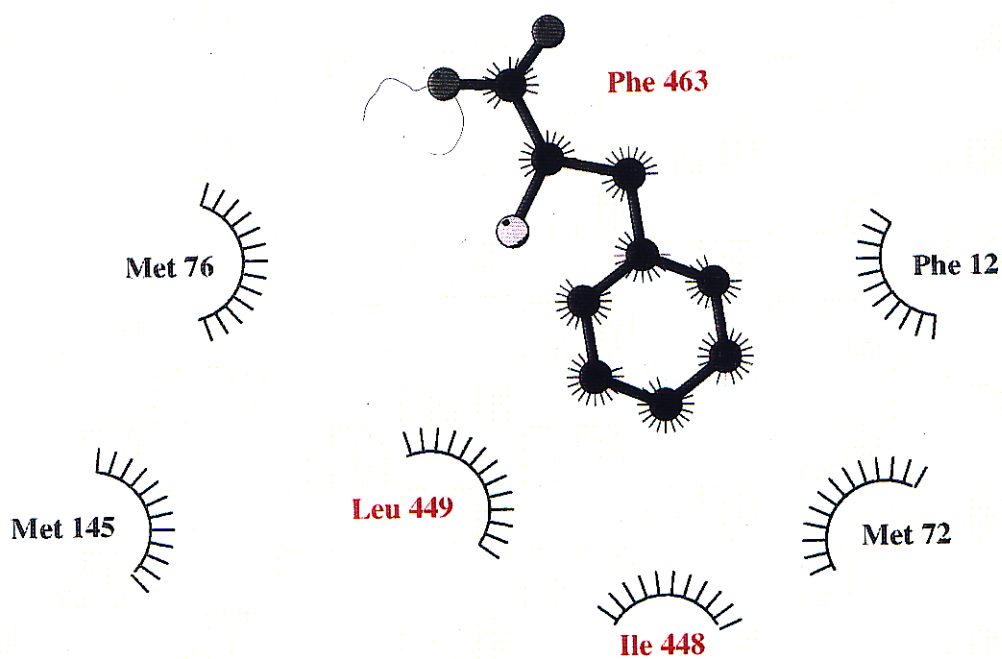
Figure II–6. Schematic drawing of the intra–molecular interations that surround and stabilize Phe 463. Residues of Ca^{2+}/CaM and CaMKK are shown in black and red, respectively.

Table II-2. R.M.S. deviations (Å) for backbone superpositions
between the individual domains of three complexes

	CaMKK	MLCK	CaMKII
CaMKK	(2.53)	1.79	2.59
MLCK	(1.92)	(0.84)	1.92
CaMKII	(1.14)	(1.92)	(2.53)

Values in parentheses are the R.M.S. deviations for superposition of the
N (residues 11-73) and C-terminal (residues 84-146) domain of one
complex on the C and N-terminal domain, respectively, of the other
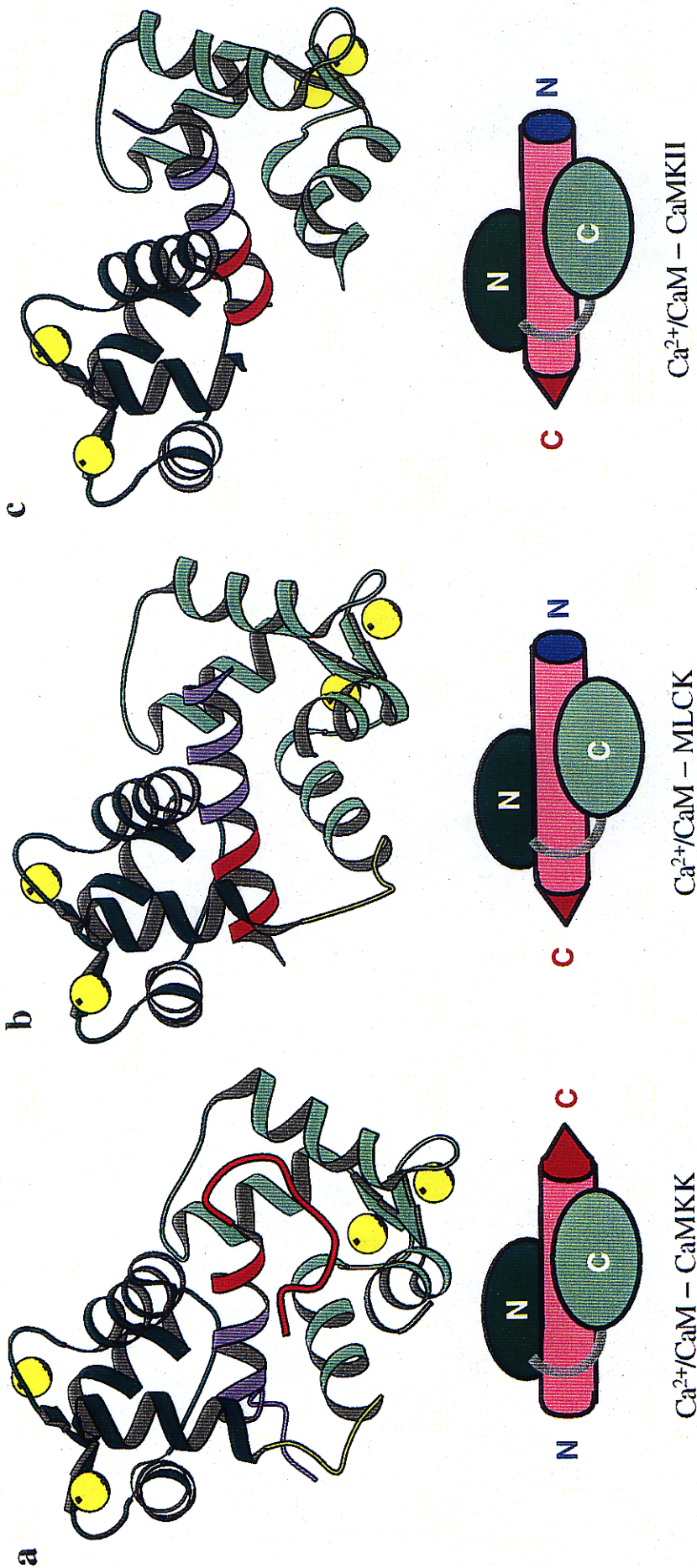complex.

Figure II-7. Ribbon drawing of Ca^{2+}/CaM complexed with a, the CaMKK, b, the MLCK (Ikura et al., 1992), and c, the CaMKII (Meador et al., 1993) peptide. CaM N-terminal domain of each complex is aligned in the same orientation. N and C-terminal halves of the target peptide are shown in blue and red, respectively. N and C-terminal domains of Ca^{2+}/CaM are shown in dark and light green with blue and red balls at N and C-terminus of Ca^{2+}/CaM, respectively. Domain linker of Ca^{2+}/CaM is in yellow. Yellow spheres are calcium ions. The ribbon diagrams were generated using MOLSCRIPT (Kraulis, 1991).

Figure II–8. Electrostatic potential surfaces of CaM (upper) and the peptide (lower) in the Ca²⁺/CaM–target peptide complexes. In upper panels, the backbone structure of the target peptide is also drawn as white tube. The surface is colored according to the local electrostatic potential, with blue and red representing positive and negative potential, respectively. a, Ca²⁺/CaM–CaMKK complex; b, Ca²⁺/CaM–smMLCK complex (Meador *et al.*, 1992); c, Ca²⁺/CaM–CaMKII complex (Meador *et al.*, 1993). This figure was generated using GRASP (Nicholls *et al.*, 1991).
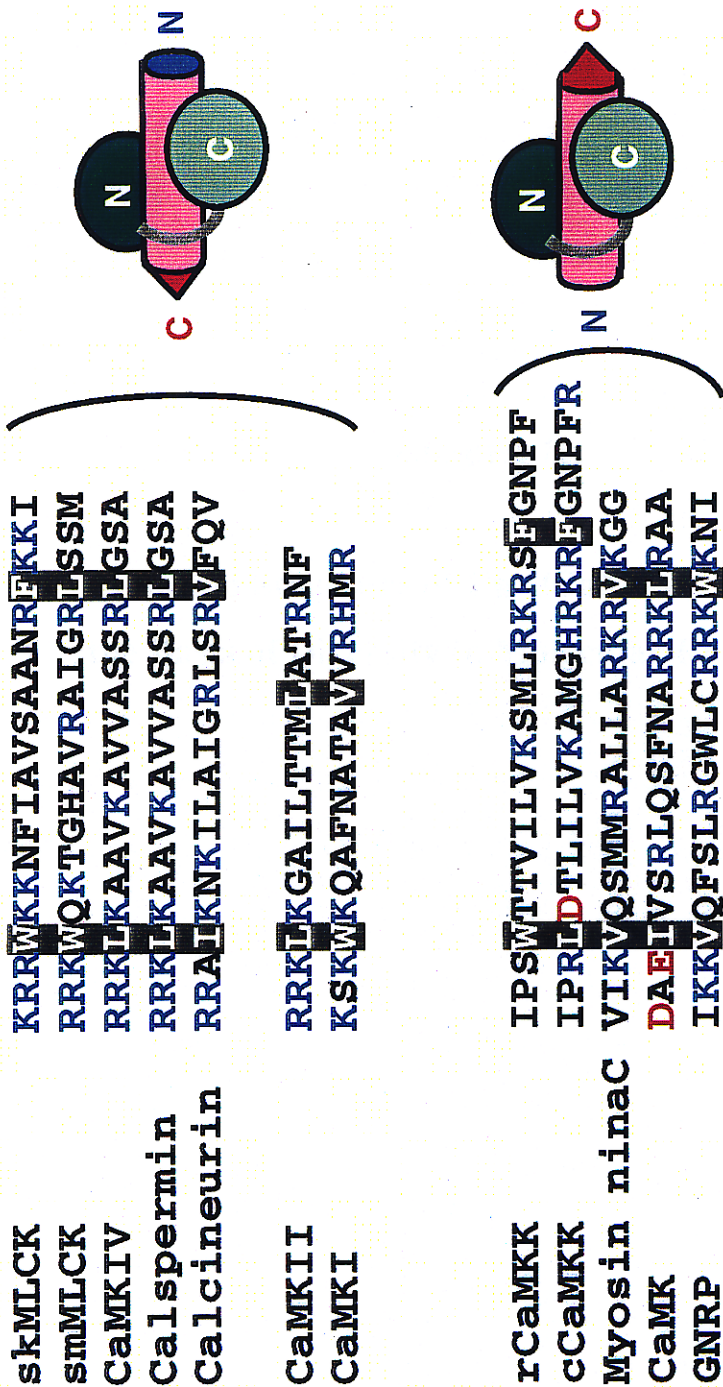
Figure II–9. Alignment of the sequences of CaM binding region based on the position of the N–terminal key residue. Key residues are shaded. Acidic and basic residues are shown in red and blue, respectively. Sequences for MLCKs, CaMKII, and CaMKKs are the same as Figure II–1a. Other sequences exept for stated are taken from the reference of Rhoads and Friedberg (Rhoads & Friedberg, 1997): rat CaMKI (residues 300–317, Goldberg *et al.*, 1996), mouse CaMKIV (residues 322–341); rat calspermin (residues 17–36); *N. crassa* calcineurin (residues 409–428); *D. melanogaster* myosin ninaC (residues 1043–1062); *M. domestica* CaMK (residues 322–341); rat guanine nucleotide releasing protein (GNRP, residues 209–228). In the right, observed or predicted binding polarity of these sequence is schematically depicted.